Characteristics Analysis and Process Study of Electroless Plating Metals Based on Computer Simulation Technology

Ruibo Duan

Yunnan College of Foreign Affairs & Foreign Language, KunMing 651700, China
527369792@qq.com

In order to realize the transformation from qualitative research to quantitative research of electroless plating, computer simulation technology has been applied in the characteristic analysis of electroless plating metals. This paper adopts the statistical simulation method, takes the process of atomic deposition in amorphous electroless nickel-phosphorus plating as the research object, establishes a computer simulation model to simulate the migration and deposition of adatoms, and analyzes its influence on the microscopic pores of the coating. The research results show that there is a negative correlation between the migration probability and migration distance of the adatoms and the microscopic porosity of the coating. As the migration probability and migration distance increase, the probability of atoms filling the pores is larger, and the pores of the coating are smaller and the quality is higher. The computer simulation study in this paper is an effective supplement to the study of the deposition process of electroless plating, and it provides a theoretical basis for the study of the microstructure of metal coating.

1. Introduction

Using chemical, mechanical, electroplating and other methods to perform surface treatment on metals or objects can achieve aesthetic, corrosion-resistant, high-wear resistance and other process requirements (Kobayashi and Lizmarzán, 2001). These coating technologies are widely used in the automotive machinery manufacturing, computer electronics technology, petrochemical, aerospace and other industries. Among them, electroless plating has been widely used for its advantages such as uniform surface coating, high economic efficiency, environmental protection and energy saving (Ang et al., 1999). As a high-temperature coating technology for surface low temperature strengthening, the electroless nickel-phosphorus plating has been widely studied and paid attention to.

The most important issue in the electroless metal plating process is the microscopic pores distribution of the coating. Domestic and foreign scholars have carried out different types of chemical experiments by changing different catalytic reducing agents and changing the acidic or alkaline concentration of the chemical solution. There are few simulation studies on the migration and deposition of the coating metals during the electroless plating process (Cheng et al., 2005). Although the qualitative optimization of the coating process has been realized macroscopically, it is urgent to study the microstructure of the coating from a microscopic point of view and perform quantitative analysis on it.

Based on the statistical simulation method (Monte Carl), this paper selects the migration and deposition process of the metal atoms in the amorphous electroless nickel-phosphorus plating as the research objects, and establishes a computer simulation model (Kikuchi et al., 2000). Through computer two-dimensional simulation, the correlation between atom migration, deposition and microscopic porosity of the coating is obtained. The experimental conclusion has certain theoretical significance for guiding the development of electroless nickel-phosphorus plating process.

2. Electroless metal plating computer model and method

2.1 Analysis of migration and deposition of adatoms

The NiL in the amorphous electroless nickel-phosphorus plating randomly collides with the $H_2PO_2^-$ chemical solution and the metal interface and surface, occurs adsorption, gains electrons and performs reduction reaction, and then the adatoms can be obtained (Yeung et al., 1999). Under certain deposition probability P_{des}, the above-mentioned adatoms will gradually deposit on the surface of the substrate, but due to the influence of atom migration during the deposition process, the adatoms will migrate relative to the initial adsorption position. Under the traction of the internal energy of the adatoms, within the maximum migration distance, the adatoms will deposit in the position where the binding energy is the highest and the coordination number is the largest, as shown in Figure 1.
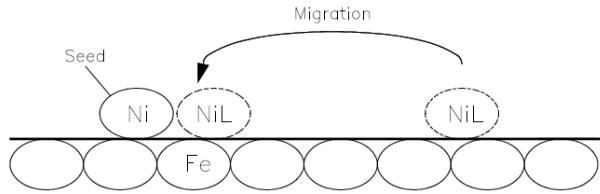

Figure 1: The migration and deposition of an adatom

In this computer simulation technology experiment, low carbon steel was used as the metal substrate surface. In the two-dimensional computer simulation, the initial deposition surface was replaced by a smooth curve, and the nickel atom was placed on the substrate surface as a random seed, the adatoms and the iron atoms on the surface occur adsorption, and the binding energy of this time is shown in Formula 1 below:

$$E_b = -\sum_j u_{ij} = -\sum_j 4\varepsilon_{ij} \left[\left(\frac{\sigma}{r}\right)^{12} - \left(\frac{\sigma}{r}\right)^6\right] \tag{1}$$

u_{ij} represents the potential energy between the adatom i and the surface atom j, σ represents the diameter of the adatom; r represents the distance between the adatom and the iron atom; ε_{ij} is the trap depth coefficient, which is related to the property of the atom (Bi et al., 2009). In the process of amorphous electroless nickel-phosphorus plating, the cut-off distance is $2\sigma_{Ni}$. Since the iron atoms have similar properties to nickel atoms, their trap depth coefficients are the same. The trap depth coefficients of nickel, iron and phosphorus are $\varepsilon_{NiFe} = 1.0$, $\varepsilon_{PFe} = 0.5$, $\varepsilon_{PP} = 0.1$, respectively. Calculating the binding energy of every Ni atom and Fe atom within the cut-off distance to obtain the total binding energy E_{ab}, then the deposition probability of nickel atoms is:

$$P_{dep} = kE_b \tag{2}$$

After initial deposition of adatoms on the surface, the surface will no longer be uniform, and the probability of deposition of this location for subsequent atoms to be deposited will be less than the overall random probability (Skandan et al., 2010). For subsequent adatoms, when the deposition probability of the atom is less than the generated random number, the adatom is deposited at the initial adsorption location; otherwise, it will migrate along the surface of the metal substrate. When the given maximum migration distance S is greater than the migration distance of the adatom; it will deposit next to the seed, so the deposition probability of this location is the largest. The subsequent adatoms are deposited in this order according to this principle; when the initial surface is completely covered by the deposited Ni atoms and P atoms, the adatoms to be deposited will no longer react with the Fe atoms, but only react with the deposited Ni atoms and the P atoms (Chen et al., 1998).

2.2 Deposition location of the adatoms

In the actual electroless plating process, the atoms are all elastic spheres, so there is a certain degree of compression and gap. The X-ray absorption fine structure (XAFS) is used to test the structural parameters of the amorphous electroless nickel-phosphorus plating layer, and then calculate the average distance of the atoms, Figure 2 shows the radial structure function of the experimental sample.
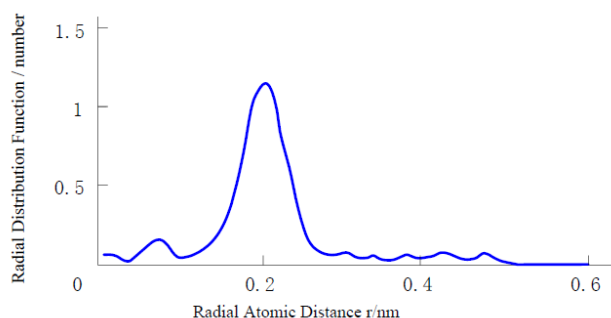
Figure 2: Radial structure function

It can be seen from the figure that the relationship between the relative intensity and the radial atom distance exhibits a normal distribution, in which the Ni-Ni and Ni-P central atom paired deposition locations are at 0.261 nm and 0.229 nm, respectively (Wang et al., 2013).

2.3 Computer simulation steps

The periodic boundary conditions are taken as the boundary conditions for the migration of coating atoms on the surface of the metal, in the computer simulation process, a roundness is used to approximately replace an adatom, and the actual atomic radius is taken as the radius. The radius of nickel atom is rN_i=0.25nm, and the radius of phosphorus atom is rP=0.22nm. For the common nickel-phosphorus coating, the ratio of nickel atom to phosphorus atom is 8:2, so this paper also uses the atom ratio of 8:2, the nickel atom is taken as a standard to determine the length as 1, the distance between phosphorus atoms $\sigma_P = \sigma_P/\sigma_{N_i}$=0.88, the coordinate length is between [0,1]. Different adsorption probability and migration probability are selected during the simulation process for the research (Barrozo et al., 2018). The steps of computer simulation are as follows:

(1) The surface length l^* is normalized to obtain the size within the standard value range. Atom diameters σ_P, σ_{N_i}, ratio of the number of Ni atoms to P atoms n, maximum migration distance S, deposition coefficient k (migration coefficient is 1-k).

(2) Generate a random number random-1 uniformly distributed in the interval [0, 1]. If the random number is less than or equal to 0.8, the nickel atom is adsorbed to form a large circle of *NiL*; if the random number is less than 0.8, the phosphorus atom is adsorbed to form a small circle (phosphite ions are adsorbed) (Carillo et al., 2018).

(3) Generate random-2 within the interval [0,1], random-2 determines the x-axis coordinate of the random number generated in step 2, and this coordinate is the same as random-2, such as if random-2=0.56, then the x-axis coordinate of the adatom generated in step 2 is 0.63 (Lee et al., 2006).

(4) Calculate the binding energy of the adatom and its deposition probability P_{dep} according to Formulas 1 and Formulas 2. When the binding energy of a phosphorus atom to a neighboring atom is 0, then random-3 is generated. When random-3 is smaller than the deposition probability, this atom migrates along the metal substrate surface, and the probabilities of migration of the adatom to both sides are the same, and the adatom will eventually be deposited within the maximum migration distance S, and the coordination number at the deposition location is the largest. In the computer simulation experiment, the average value of the adatom random number is calculated to be 1.122σ, and the variance is 0.33, which satisfies the normal distribution, and then determine the height coordinate y of the adatom (Lee et al., 2018).

(5) Repeat steps 2 and 4 to statistically classify each set of adatom coordinates to calculate the radial distribution function and microscopic porosity (Yu et al., 2018).

3. Computer simulation results and analysis

3.1 Calculation of simulation results

The results of the computer simulation process of electroless plating metal atoms can be evaluated by using graphs and porosity as indicators. The calculation formula for the porosity is as Formula 3 below:

$$V = \frac{S_V}{S_{all}} \tag{3}$$

S_V is the pore area of the coating, and S_{all} is the total area of the coating, respectively give different *k* and S values to get different calculation results. Figure 3 shows the two-dimensional computer simulation graph with different atom migration probability k, maximum migration distance S and microscopic porosity.
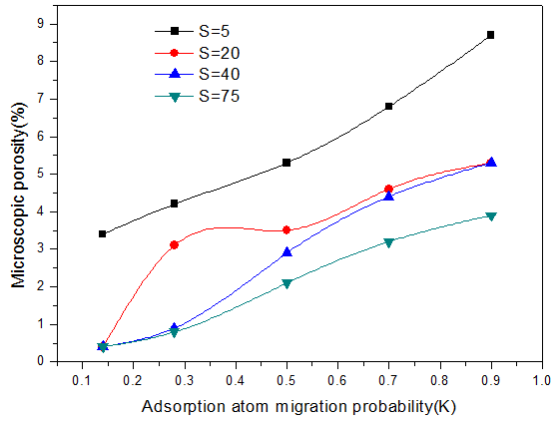

Figure 3: The Relationship between k, S and microscopic porosity

It can be seen from the figure that the microscopic porosity of the amorphous nickel-phosphorus plating decreases with the increase of the probability of migration, and decreases with the increase of the maximum migration distance (Fan, Q. et al., 2018).

3.2 Verification of computer simulation results

In this section, the empirical formula is used to verify the results of computer simulated electroless plating, mainly using the radial distribution function RDF and density as two indicators.

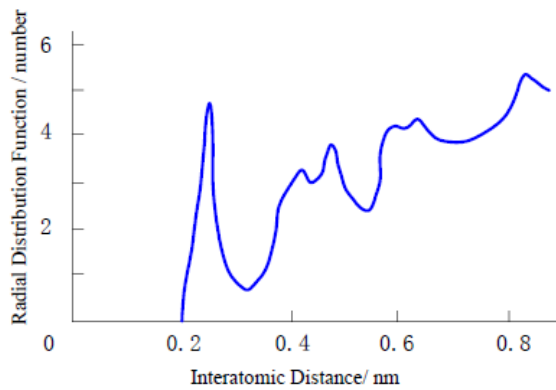### 3.2.1 Radial distribution function (RDF)

Figure 4: The RDF shape features

RDF is three-dimensional, and this computer simulation is to simulate the two-dimensional cross section of the coating. Therefore, at first, we need to define the RDF of the two-dimensional section. Referring to the definition of the RDF, RDF is the average number of atoms distributed on a sphere with a radius of r and an atom as the center of the sphere, so we can define the two-dimensional cross section RDF as: the average number of atoms distributed on a sphere with a radius of r and an atom as the center of the sphere, represented by RDF_2, its formula is shown as Formula 4:

$$RDF_2 = 2\pi r \rho(r) \tag{4}$$

$\rho(r)$ is the probability of atoms distributed on the circumference of radius r. Figure 4 shows the graph of simulated RDF_2.

It can be seen from the figure that the shape of RDF of the metal coating is similar to that of the amorphous material, and the relationship between the RDF and the distance between atoms presents a state of the amorphous material, thus verifying that the atom distribution of the nickel-phosphorus coating is an amorphous structure.

3.2.2 Density

Although the RDF qualitatively demonstrates that the computer simulation results presented an amorphous state characteristic, it still needs to be verified in quantitative terms. The simulation results were verified by density test. For a given surface length l, according to the computer simulated atom number, we can calculate the mass of the atom set. The volume of the atom is the volume when we approximately consider the atom as a sphere with the thickness of the model as the diameter of the atom. Under the above assumptions, the density of the simulated graph is calculated as $\rho = 7.34 \, \text{g.} \, cm^{-3}$, and the density of the compound metals of the coating in the actual amorphous nickel-phosphorus plating is $7.68 \, \text{g.} \, cm^{-3}$, the relative error is only 4.4%. Analyzing computer simulation results from a quantitative perspective has a high precision.

3.3 Analysis and discussion

3.3.1 Relationship between atom migration probability and microscopic porosity

During the migration process, atoms will have different deposition and growth locations on the metal substrate surface. Different migration probabilities will lead to different coating structures, and finally these two would affect the pore structure of the metal coating together. The probability of atom migration is related to atom migration. The possibility that atoms with low migration probability remain in the initial location is large, causing most of the atoms to deposit at the initial location. Minor atoms deposit at the locations where there are more matching positions, and the overall porosity of the coating increases. When the migration probability increases, the microscopic porosity decreases, there is a negative correlation.

3.3.2 Relationship between migration distance of adatoms and the microscopic porosity

The maximum migration distance affects the ability of atoms to fill pores and holes in farther locations, so a larger migration distance of the adatoms is more favorable for the microscopic structure of the pores of the coating. If the migration distance of the adatoms is small, the microscopic structure and density of the coating will decrease. The migration distance becomes larger, the microscopic porosity of the coating decreases, there is also a negative correlation.

4. Conclusion

Electroless plating has been widely used in metal plating processes due to its high coating quality, environmental protection, high economic efficiency, etc. Domestic and foreign scholars have carried out various types of experiments and researches on the electroless plating process. There are many experimental studies on plating solution performance, coating deposition speed and coating hardness parameters, while there are few researches using computer simulation to study the atom migration and deposition characteristics in electroless plating process. This paper had taken this condition as an opportunity for the study. The main research contents and conclusions of this paper are as follows:

(1) This paper took amorphous nickel-phosphorus plating as the research object, and used computer simulation method to quantitatively analyze the microscopic characteristics of the coating.

(2) This paper established a computer simulation method for electroless nickel-phosphorus plating, and analyzed the migration probability k and migration distance S of the adatoms.

(3) As the migration probability and migration distance of the adatoms increase, the ability of coating atoms to fill the holes and pores will be improved, and the microscopic porosity of the coating reduces accordingly.

References

Barrozo F.B., Valencia G.O., Cardenas Y.E., 2018, Computational simulation of the gas emission in a biomass on grid energy system using homer pro software, Chemical Engineering Transactions, 65, 265-270, DOI: /10.1016/j.proeng.2015.11.408

Bi H., Kou K.C., Rider A.E., Ostrikov K., Wu H.W., Wang Z.C., 2009, Low-phosporous nickel-coated carbon microcoils: controlling microstructure through an electroless plating process, Applied Surface Science, 255(15), 6888-6893, DOI: /10.1016/j.apsusc.2009.03.009

Carillo P., D'Amelia L., Dell'Aversana E., Faiella D., Cacace D., Giuliano B., 2018, Eco-friendly use of tomato processing residues for lactic acid production in campania, Chemical Engineering Transactions, 64.

Chen W., Li L., Qi J., Wang Y., Gui Z., 1998, Influence of electroless nickel plating on multilayer ceramic capacitors and the implications for reliability in multilayer ceramic capacitors, Journal of the American Ceramic Society, 81(10), 2751-2752, DOI: /10.1111/j.1151-2916.1998.tb02693.x

Cheng K., Yang M.H., Chiu W.W.W., Huang C.Y., Chang J., Ying T.F., 2005, Ink-jet printing, self-assembled polyelectrolytes, and electroless plating: low cost fabrication of circuits on a flexible substrate at room temperature, Macromolecular Rapid Communications, 26(4), 247–264, DOI: /10.1002/marc.200400462

Fan Q., Gao Y., Zhao Y., Yang Q., Guo L., Jiang L., 2018, Fabrication of diamond-structured composite materials with ni-p-diamond particles by electroless plating, Materials Letters, 215, 242–245, DOI: /10.1016/j.matlet.2017.12.065

Kikuchi E., Nemoto Y., Kajiwara M., Uemiya S., Kojima T., 2000, Steam reforming of methane in membrane reactors: comparison of electroless-plating and cvd membranes and catalyst packing modes, Catalysis Today, 56(1–3), 75-81, DOI: /10.1016/s0920-5861(99)00264-3

Kobayashi Y., Lizmarzán L.M., 2001, Deposition of silver nanoparticles on silica spheres by pretreatment steps in electroless plating, Chemistry of Materials, 13(5), DOI: /10.1021/cm001240g

Lee H., Jung J., Heo C., Kim C., Lee J.H., Kim Y., 2018, Characterization of the contamination factor of electroless ni plating solutions on the enig process, Journal of Electronic Materials, 1-7, DOI: /10.1007/s11664-018-6335-1

Lee K.H., Lee J., Chang H.W., Che W.S., 2006, Computing current density distribution for plating on plastic parts using computer simulation, Electrochemical Society.

Liming Ang T.S.A.H., Xu G.Q., Tung C., Zhao S.P., Wang J.L.S., 1999, Electroless plating of metals onto carbon nanotubes activated by a single-step activation method, Chemistry of Materials, 11(8), 2115-2118, DOI: /10.1021/cm990078i

Skandan G., Glumac N., Chen Y.J., Cosandey F., Heims E., Kear B.H., 2010, Low‑pressure flame deposition of nanostructured oxide films, Journal of the American Ceramic Society, 81(10), 2753-2756, DOI: /10.1111/j.1151-2916.1998.tb02694.x

Wang M.Q., Yan J., Du S.G., Zeng J.W., Chang W.P., Guo Y., 2013, Adsorption characteristic of copper ions and its application in electroless nickel plating on a hydrogel-functionalized poly (vinyl chloride) plastic, Journal of Materials Science, 48(20), 7224-7237, DOI: /10.1007/s10853-013-7539-7

Yeung K.L., Christiansen S C., Varma A., 1999, Palladium composite membranes by electroless plating technique: relationships between plating kinetics, film microstructure and membrane performance, Journal of Membrane Science, 159(1–2), 107-122.

Yu Q., Zhou, T., Jiang, Y., Yan X., An Z., Wang X., 2018, Preparation of graphene-enhanced nickel-phosphorus composite films by ultrasonic-assisted electroless plating, Applied Surface Science, 435, 617-625, DOI: /10.1016/j.apsusc.2017.11.169